

Building integrated photovoltaic modules and the integration of phase change materials for equatorial applications

Building Serv. Eng. Res. Technol.
2020, Vol. 41 (5) 634–652

© Authors 2019

Article reuse guidelines:

sagepub.com/journals-permissions

DOI: 10.1177/0143624419883363

journals.sagepub.com/home/bse



A Karthick¹ , K Kalidasa Murugavel²,
K Sudalaiyandi² and A Muthu Manokar³

Abstract

The performance of building integrated photovoltaic (BIPV) system depends on the geographical location and the incident angle of solar radiation. In this paper, a simple mathematical model has been developed to predict the performance of BIPV modules with and without phase change material (PCM). The effect of transmittance of the BIPV glass cover is studied with respect to incident solar radiation. The performance curves, annual energy and exergy gains are analysed for hot and humid climatic conditions of Kovilpatti (9°10'0"N, 77°52'0"E), Tamil Nadu, India. The annual electrical energy gains of the BIPV-PCM for the south orientation is (135 kWh) and the east orientation (110 kWh) obtained the minimum. Similarly, the annual electrical energy of the BIPV-PCM is maximum in the east orientation and minimum in the west orientation. The south orientation BIPV-PCM obtained the maximum energy (190 kWh) and exergy (27.3 kWh). The theoretically calculated results have good agreement with experimental results.

Practical application: Integration of photovoltaic modules into the building structure has many benefits and challenges; before integrating into the building structure, the performance and impact of the BIPV module needs to be studied. This study will assist developers and designers to understand the likely performance of the BIPV modules and assess the benefit of integrated phase change materials for application in residential buildings in equatorial climate zones.

Keywords

Building integrated photovoltaic, building integrated photovoltaic phase change material, Facade, Glauber salt

¹Department of Electrical and Electronics Engineering, KPR Institute of Engineering and Technology, Anna University, Tamil Nadu, India

²Centre for Energy Studies, Department of Mechanical Engineering, National Engineering College, Anna University, Tamil Nadu, India

³Department of Mechanical Engineering, B.S. Abdur Rahman Crescent Institute of Science and Technology, Chennai, India

Corresponding author:

A Karthick, KPR Institute of Engineering and Technology, Avinashi Road, Arasur, Coimbatore 641407, Tamil Nadu, India.
Email: karthick.power@gmail.com

Introduction

Building integrated photovoltaic (BIPV) is an emerging technology for harnessing the solar energy, and it also reduces the lighting, heating and cooling load. Solar photovoltaic (PV) cell could convert 5–25% of the incident solar radiation into electricity and the remaining energy is converted into heat.¹ Ramanan et al.¹ investigated the performance of the PV modules on hot and humid climatic condition. It was reported that the output power of the PV modules varies with respect to incident solar radiation and the surface temperature of the PV cells. The solar water heater and BIPV products can be used for building applications by being integrated into elements of the building envelope, such as roof, façades, and skylights.^{2–3} The challenges in the integration of the BIPV modules on facades, roof and skylights were presented.⁴ The surface temperature of the module is controlled by various cooling methods, such as active and passive cooling. The passive cooling plays a vital role in the cooling of the BIPV systems. The energy consumption and cost of the system is lower compared to active cooling method. The passive cooling methods are classified as phase change material (PCM) and wicking materials.⁵

The air-based cooling approach is the active cooling method which blows air to reduce the surface temperature of PV module by natural ventilation. The heat transfer rate of the module is enhanced by increasing heat transfer area using fins.⁶ Yun et al.⁷ investigated the performance of PV façade with ventilation and without ventilation. It revealed that the peak surface temperature of PV panel with ventilation obtained 55.5°C in comparison to 76.7°C for the PV module without ventilation. The incorporation of PCM in the BIPV modules is a challenging task due to the phase transition process as it changes from solid to liquid and liquid to solid. Most widely used methods for assimilation of PCM in BIPV has been presented in the literature.^{8–10} The performance of the BIPV module with various PV cell coverage ratios was analysed. It was reported that the performance of

the BIPV module was higher for the lesser cell coverage ratio.¹¹ Karthick et al.¹² investigated the performance of the BIPV module with and without PCM. It was reported that the incorporation of inorganic PCM Glauber salt reduced the surface temperature of the module up to 8°C compare to the conventional BIPV module. It also revealed that the incorporation of the PCM improved the system efficiency by 10%.

Royo et al.¹³ presented a mathematical model to predict the performance of BIPV modules. It was reported that the system with PCM reduced the temperature up to 7.5°C compared to reference BIPV system. Biwole et al.¹⁴ performed a numerical study in PV-PCM and reported that the system with PCM maintained the surface temperature up to 40°C for 80 min, while the PV without PCM module at 40°C for 5 min. Elarga et al.¹⁵ reported that the implementation of a PCM layer in the semi-transparent PV façade could reduce the cooling energy demand of the buildings up to 30% for the locations in Abudhabi, Venice and Helsinki. Barman et al.¹⁶ investigated the performance of cadmium telluride semi-transparent photovoltaic (STPV) window system for a composite climatic region in India. It is reported that the STPV window have potential to generate 119.6 kWh/m²/year. Wang et al.¹⁷ compared the performance of the PV double skin façade and PV insulating glass unit. The result indicated that the PV double skin façade performance was 1.8% better than the PV insulating glass unit in terms of reduction in solar heat gain, and also the energy saving potential of both the systems is higher compared to the conventional windows. Debbarma et al.¹⁸ reviewed thermal model, energy and exergy analysis specifically for BIPV systems. It was concluded that the BIPV system can fulfil the partial energy requirements of the building. However, developments are needed in BIPV technologies to reduce the cost of the system. Hasan et al.¹⁹ investigated the paraffin-based PV-PCM system and reported that the output power of the PV module was increased by 5.9% compared to the conventional PV module in the hot climatic zones of United Arab Emirates.

The performance of the BIPV system varies depending upon the geographical location. From the literature studies, it was found that thermal modelling for BIPV and BIPV-PCM had been investigated thoroughly for the past two decades but it remains as a challenging task. Few researches have been reported for the Indian climatic conditions, such as the thermal model of BIPV system for composite climatic conditions²⁰ and the experimental investigation of the BIPV façades^{11,12} for hot and humid climatic conditions. However, research on the thermal modelling and energy gains of the BIPV and BIPV-PCM system for hot and humid climatic in the region of India is seldom found. Before integration into building structures, the performance of BIPV system needs to be predicted. The objective of this work is to estimate the electrical and thermal gain of the BIPV module with and without PCM. The simple mathematical model is developed for the prediction, to estimate the year round energy and exergy gain of the module using solar radiation, ambient temperature data and the thermophysical properties of the PCM.

Objectives and methodology

The objective of this work is to develop the simple model to predict the performance of the BIPV system with and without PCM. The specification of the BIPV modules used for the design is obtained from the work of Karthick et al.¹¹ The design parameters used in this study for energy analysis is given in Table 1. To predict the annual electrical, thermal energy and exergy gain of the system, the following methodologies have been adopted. In addition, the hourly variation of ambient parameters for various orientations, surface temperatures, electrical parameter of modules and instruments used have been conferred. The overall layout of the study is presented in Figure 1.

- (i) The hourly ambient air temperature and beam radiation on horizontal surface have been obtained from our meteorological station and installed in our campus, National

Table 1. Design parameters of building-integrated photovoltaic systems.

Parameter	Value
A_f	18m ²
A_m	0.69 m ²
C_a	1005 J/kgK
h_0	5.7 W/m ² K
h_c	2.8 W/m ² K
h_i	2.8 W/m ² K
K_g	0.9 W/mK
K_r	0.67 W/mK
L_g	0.004 m
L_r	0.6 m
N	4
T_{ref}	25°C
T_s	6000 K
V	28 m ³
v	0
α_c	0.9
α_r	0.4
β	0.62,0.72,0.82
ρ_{air}	1.2 kg/m ³
τ_g	0.7
Inclination	90°

Engineering College, Kovilpatti, Tamil Nadu, India. Further, beam radiation has been calculated at 90° inclination for vertical surface at Kovilpatti, India, by using MATLAB 2013a.

- (ii) From equations (33) and (44), the hourly rate of useful electrical energy, overall thermal energy gain and overall exergy of the system have also been evaluated.
- (iii) Daily thermal energy and exergy and electrical gain have been calculated by summing the hourly rate of useful thermal and exergy and electrical gain.
- (iv) Carbon credits have been calculated annually on an overall energy and exergy basis. The CO₂ emission reduction per annum from BIPV on annual overall energy basis and exergy basis has been calculated using

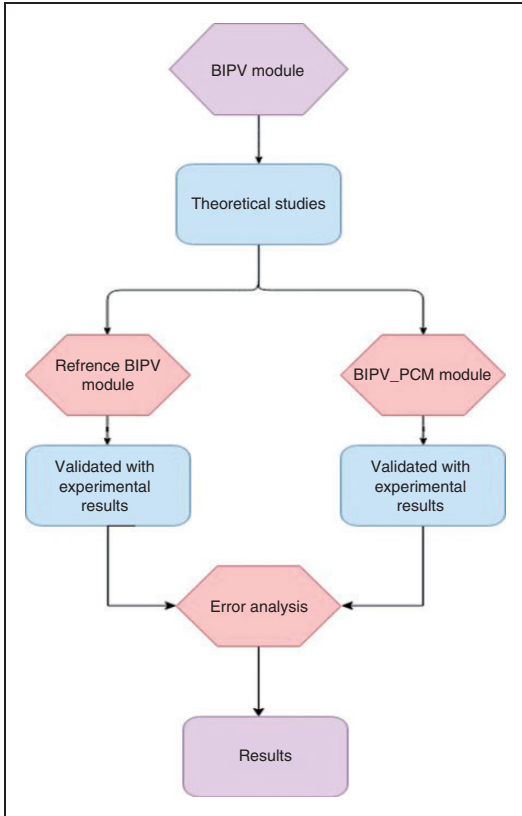


Figure 1. Overall layout of the study.

equation (47). The enviro-economic cost parameter, the CO₂ mitigation price per annum is evaluated by equation (48).

Theoretical framework of the BIPV module

The thermal modelling of the studied system is based on the heat balance equations (energy conservation principle) for each component of the solar device. In order to write the energy balance equations for BIPV modules, the following assumptions have been made: the experimental setup shown in Figure 2 is the work of inorganic PCM used by Karthick et al.¹² which has a melting point of 32°C and latent heat of 251 kJ/kg, respectively. PCM is incorporated at



Figure 2. Photographic view of the experimental room.

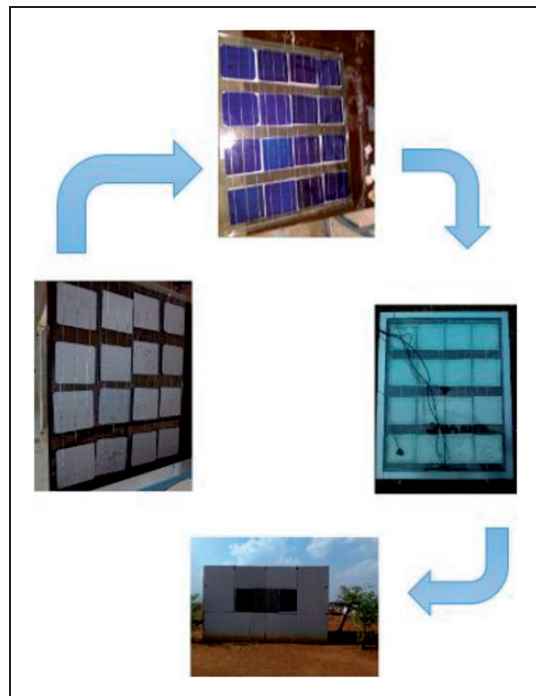


Figure 3. Fabrication process of BIPV module with and without PCM.

the rear side of the module to enhance the heat transfer rate of the module and it is tightly encapsulated. The fabrication process of BIPV and BIPV-PCM module is shown in Figure 3.

The overall flow chart of the study is presented in Figure 4.

- One-dimensional heat conduction is a good approximation.

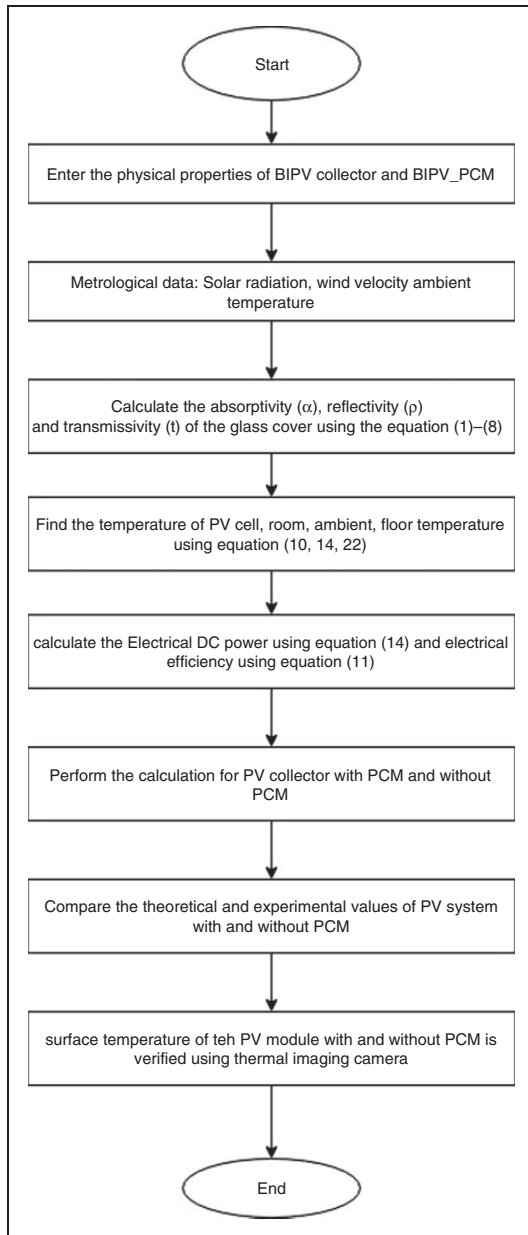


Figure 4. Flow chart of the analysis procedure.

- The system is in quasi-steady state and the ohmic losses in the solar cell is negligible.
- The initial temperature of the BIPV is the same as that of the PCM and heat transfer occurs mainly by natural convection and heat conduction.
- We neglect the thermal exchanges between PCM and walls and between PCM and PV cells.
- PCM is non-reactive and homogeneous, and there is no heat loss from the top and bottom adiabatic boundaries.
- The ambient temperature is postulated as equal on all sides of the module.

Transmissivity of the glass

The transmissivity of the STPV glass cover can be obtained by reflection–refraction and absorption discretely and it is expressed by Suhatme et al.²¹

$$\tau_g = \tau_r * \tau_a \quad (1)$$

According to Snell's law

$$\frac{\sin \theta_1}{\sin \theta_2} = \frac{n_2}{n_1} \quad (2)$$

The reflectivity (λ) is related to the angle of incidence and refraction

$$\lambda = \frac{1}{2}(\lambda_1 + \lambda_2) \quad (3)$$

$$\lambda_1 = \frac{\sin^2(\theta_2 - \theta_1)}{\sin^2(\theta_2 + \theta_1)} \quad (4)$$

$$\lambda_2 = \frac{\tan^2(\theta_2 - \theta_1)}{\tan^2(\theta_2 + \theta_1)} \quad (5)$$

$$\tau_r = \frac{1 - \lambda}{1 + \lambda} \quad (6)$$

$$\tau_a = e^{-Kl / \cos \theta_2} \quad (7)$$

$$\tau_g = \left(\frac{1 - \lambda}{1 + \lambda} \right) * e^{-Kl / \cos \theta_2} \quad (8)$$

Equations (7) and (8) are substituted into equation (1) to estimate the transmissivity of the semi-transparent PV module glass cover.

Glass-to-glass PV module

According to Vats and Tiwari,²² the energy balance equation for solar cell of BIPV module can be written as

$$\begin{aligned} \tau_g \alpha_c \beta_c I \Delta t A_m &= [U_{tc,a}(T_{pv} - T_a) \\ &+ U_{tc,r}(T_{pv} - T_r)] A_m \\ &+ \tau_g \alpha_c \eta_{elec} \beta_c I \Delta t A_m \end{aligned}$$

$$\left[\begin{array}{l} \text{rate of} \\ \text{solar energy} \\ \text{absorbed by} \\ \text{BIPV module} \end{array} \right] = \left[\begin{array}{l} \text{overall} \\ \text{heat loss} \\ \text{from top surface of} \\ \text{solar cell} \\ \text{to ambient} \end{array} \right] + \left[\begin{array}{l} \text{overall} \\ \text{heat loss} \\ \text{from the} \\ \text{back side of the} \\ \text{solar cell} \\ \text{to room} \end{array} \right] + \left[\begin{array}{l} \text{rate of} \\ \text{electrical} \\ \text{energy} \\ \text{produced} \end{array} \right] \quad (9)$$

From equation (9), the solar cell temperature is derived

$$T_{pv} = \frac{\tau_g \beta_c (\alpha_c - \eta_{elec}) I \Delta t + U_{tc,a} T_a + U_{tc,r} T_r}{U_{tc,a} + U_{tc,r}} \quad (10)$$

Evans²³ derived an expression for an electrical efficiency of a PV module to calculate the standard test conditions (25°C, 1000 W/m²) which is dependent on temperature. The expression is

$$\eta_{elec} = \eta_o [1 - \beta_o (T_{pv} - T_{ref})] \quad (11)$$

$$\eta_{elec} = \frac{\left\{ \eta_o [1 - \beta_o \{ \tau_g I \Delta t \beta_c \alpha_c + U_{lca} (T_a - T_{ref}) \}] + U_{lcr} (T_r - T_{ref}) \right\}}{1 - \frac{\eta_o \beta_{o\tau_g I \Delta t \beta_c \alpha_c}}{U_{lca} + U_{lcr}}} \quad (12)$$

Substituting the solar cell efficiency from equation (10) into equation (9), solar cell temperature may be calculated as

$$T_{pv} = \frac{\left\{ \tau_g I \Delta t \beta_c \{ [\alpha \tau I \Delta t]_1 - U_o (T_r - T_{ref}) \} + U_{lca} T_a + U_{lcr} T_r \right\}}{U_{lca} + U_{lcr}} \quad (13)$$

In equation (13), solar PV cell temperature is only reliant on solar radiation and room air temperature unlike the previous model equation (10) which is reliant on solar cell efficiency. The instant power delivered by the BIPV module can be calculated using the Osterwald model²⁴

$$P_{DC} = P_{m, stc} * \frac{I}{I_{ref}} [1 + \beta_m (T_{pv} - T_{ref})] \quad (14)$$

Substituting equation (13) into equation (14), the DC power of the module can be calculated with respect to incident solar radiation and room air temperature

$$P_{DC} = P_{m, stc} * \frac{I}{I_{ref}} \left[1 + \beta_m \left(\frac{\tau_g I \Delta t \beta_c \{ [\alpha \tau I \Delta t]_1 - U_o (T_r - T_{ref}) \} + U_{lca} T_a + U_{lcr} T_r}{U_{lca} + U_{lcr}} - T_{ref} \right) \right] \quad (15)$$

The energy balance equation for the floor of the room is given by Tian and Zhao²⁵ and energy balance for the room air temperature (T_r) can be written as

$$\begin{aligned} \alpha_g \tau_g^2 (1 - \beta_c) A_m I \Delta t \\ = h_c A_m (T_f - T_r) + U_b (T_f - T_o) A_m \end{aligned} \quad (16)$$

where $(1 - \beta)A_m$ is the non-packing area of BISPV module, which allows solar radiation to penetrate and enter the room. Further, equation (16) can be rewritten as

$$T_f = \frac{\alpha_g \tau_g^2 (1 - \beta_c) A_m I \Delta t + U_{bA_m} T_o + h_c A_m T_r}{(h_c + U_b) A_m} \quad (17)$$

where $0.33NV (T_r - T_a)$ is used to calculate the rate of thermal energy from the room air to the ambient in natural condition. With the help of equation (13), equations (15) and (16) can be rearranged as first-order differential equation

$$\frac{dT_r}{dt} + ST_r = f(t) \quad (19)$$

where

$$S = \frac{U_{ra} A_m + U_{beff} \beta A_m U_o I \Delta t + U_{ra} A_m + 0.33NV}{M_a C_a} \quad (20)$$

$$f(t) = \left[\frac{\left\{ \left[h_{ceff} \alpha_g \tau_g^2 (1 - \beta_c) \right] + \left\{ U_{beff} \beta [\alpha \tau I \Delta t]_1 \right\} + [T_{ref} * U_{beff} \beta U_o] I \Delta t A_m + [U_{ro} A_m T_o] [U_{ra} A_m + 0.33NV] \right\}}{M_a C_a} \right] \quad (21)$$

Energy balance for room air temperature (T_r) may be expressed as

$$\begin{aligned} M_a C_a \frac{dT_r}{dt} = h_c A_m (T_f - T_r) \\ + U_{ic,r} (T_{pv} - T_r) A_m \\ - 0.33NV (T_r - T_a) \end{aligned} \quad (18)$$

$$\left[\begin{array}{c} \text{rate of} \\ \text{thermal energy} \\ \text{absorbed} \\ \text{by the room} \end{array} \right] = \left[\begin{array}{c} \text{rate of} \\ \text{heat transfer} \\ \text{from solar cell} \\ \text{to room air} \end{array} \right] + \left[\begin{array}{c} \text{rate of} \\ \text{heat loss} \\ \text{from room} \\ \text{to ambient} \end{array} \right]$$

Equation (19) is solved considering the initial condition as: $T_r t=0 = T_{r0}$ and $f(t)$ and T_a are average values of incident solar radiation and atmosphere air temperature in the time interval. After performing the differentiation of equation (19), the solution is

$$T_r = \frac{f(t)}{a} (1 - e^{-at}) + T_{r0} e^{-at} \quad (22)$$

The room air temperature is found out from equation (18) for a given location and design specification, PV energy conversion efficiency, floor temperature and PV surface temperature can be obtained from equations (15), (12) and (13), respectively.

In the energy balance equation of the BIPV-PCM system, an additional component heat storage by the PCM is added to study the effect of incorporation of PCM. And also to

calculate the temperature difference between a BIPV reference system and a BIPV-PCM system. The energy stored in the PCM is the sum of sensible heat and latent heat. However, the contribution of sensible heat is negligible because the storage capacity of the latent heat is 200 times greater than that of sensible heat.²⁶ Some amount of heat energy generated during the operation of the solar PV cell is transferred to PCM layer through conduction process

$$\tau_g \alpha_c \beta_c I \Delta t A_m = [U_{tc,a}(T_{pvpcm} - T_a) + U_{tc,r}(T_{pvpcm} - T_r)] A_m + \tau_g \alpha_c \eta_{elec} \beta_c I \Delta t A_m + Q_{cond}$$

$$\begin{bmatrix} \text{Rate of} \\ \text{solar energy} \\ \text{absorbed} \\ \text{by the} \\ \text{solar cell} \end{bmatrix} = \begin{bmatrix} \text{Rate of} \\ \text{heat transfer} \\ \text{from} \\ \text{solar cell} \\ \text{to ambient} \end{bmatrix} + \begin{bmatrix} \text{Rate of} \\ \text{heat transfer} \\ \text{from} \\ \text{solar cell} \\ \text{to room} \end{bmatrix} + \begin{bmatrix} \text{Rate of} \\ \text{electrical} \\ \text{energy} \\ \text{produced} \end{bmatrix} + \begin{bmatrix} \text{Rate of} \\ \text{heat} \\ \text{storage} \\ \text{by the PCM} \end{bmatrix}$$

From equation (4), the solar cell temperature is derived

$$T_{pvpcm} = \frac{\tau_g \beta_c (\alpha_c - \eta_{elec}) I \Delta t + U_{tc,a} T_a + U_{tc,r} T_r - \frac{Q_{cond}}{\Delta t}}{U_{tc,a} + U_{tc,r}} \quad (24)$$

The following expressions are given by Gholampour et al.²⁷ which is used for the conduction part in three temperature-dependent states

$$Q_{cond1} = \frac{A_m k x (T_{pvpcm} - T_a)}{C_{PCM}} \quad (25)$$

for $T_a < T_{pvpcm} < T_{fusion}$

$$Q_{cond2} = \frac{A_m k x H (T_{pvpcm} - T_{fusion})}{C_{PCM}} \quad \text{for}$$

$$T_{fusion} < T_{pvpcm}, \quad \sum^k HS(T_{pvpcm} - T_{fusion}) \leq H_m \quad (26)$$

$$Q_{cond3} = \frac{A_m k x (T_{pvpcm} - T_a)}{C_{PCM}} \quad \text{for}$$

$$T_{fusion} \geq T_{pvpcm}, \quad \sum^k HS(T_{pvpcm} - T_{fusion}) \geq H_m \quad (27)$$

Equation (23) act as the base equation for the heat transfer studies in the BIPV-PCM system. The heat energy storing capacity in the PCM begins when T_{pvpcm} and T_{fusion} are equal. The phase change occurs when the T_{pvpcm} is greater than T_{fusion} which minimises the temperature difference between T_{pvpcm} and T_a . The energy storing capacity of the system may be stopped due to two reasons. When it attains the latent heat, the energy storing capacity of the PCM, or the surface temperature, drops below the T_{fusion} of the PCM. In addition, the energy discharge cycle starts and the accumulated latent heat energy begins to dissipate. During this cycle, T_{pvpcm} is higher than T_{pvpcm} until the cycle completes; this is due to fact that the energy released form the PCM increases the surface temperature of the BIPV-PCM system.

Energy and exergy analysis of BIPV modules

Electrical energy gain.

$$P_{DC} = P_{m, stc} * \frac{I}{I_{ref}} [1 + \beta_m (T_{pv} - T_{ref})] \quad (28)$$

$$\eta_{elec} = \eta_o [1 - \beta_o (T_{pv} - T_{ref})] \quad (29)$$

The Annual electrical power (W) is

$$E_{el.hourly} = \eta_{elec} X A_m X I \Delta t_{hourly} \quad (30)$$

The expression for daily electrical energy in kWh is

$$E_{el.daily} = \sum_{i=1}^S \frac{E_{el.hourly,i}}{1000} \quad (31)$$

where S is the number of sunshine hours per day. The expression for monthly electrical energy in kWh is given as

$$E_{el.monthly} = E_{el.daily} X m_o \quad (32)$$

where m_o is the number of clear days in a month. The expression for annual electrical energy in kWh is

$$E_{el,annual} = \sum_{m=1}^{12} E_{el.monthly,m} \quad (33)$$

Thermal gain. The radiation passing through the non-packing area of the cell helps in direct space heating, whereas the radiation falling on the solar cell is partially converted into electrical energy and the remainder helps in indirect space heating. Consider a room has a glass-to-glass PV array integrated into the building as a window facing the equator. The direct thermal energy gain through the non-packing area of the PV module is given by Agrawal and Tiwari²⁸

$$Q_{np} = [(1 - \beta)\tau^2 I \Delta t - h_{np}(T_{pv} - T_a)] A_m \quad (34)$$

As the thickness and thermal conductivity of the solar cells are almost equal to that of the EVA, indirect gain through the PV module packing area is given by

$$Q_p = [\beta\tau G(t) - h_p(T_{pv} - T_a)] A_m \quad (35)$$

Adding equations (22) and (23), the net heat gain through the STPV module is

$$Q = Q_{np} + Q_p \quad (36)$$

$$h_{np} = \left[\frac{1}{h_{c,a}} + \frac{l_g}{K_g} + \frac{l_g}{K_g} + \frac{1}{h_{si}} \right]^{-1} \quad (37)$$

$$h_p = \left[\frac{1}{h_{c,a}} + \frac{l_g}{K_g} + \frac{l_c}{K_c} + \frac{l_g}{K_g} + \frac{1}{h_{si}} \right]^{-1} \quad (38)$$

$$h_{pv} = h_{np} + h_p$$

The total thermal gain through a module during sunshine hours is given by

$$Q_{Th} = \sum_{i=1}^N \int_0^{t_{tr}} Q d \quad (39)$$

$$Q_{Th} = h_{pv} \left[\frac{\{(1 - \beta)\tau + \beta\}\tau\{I \Delta t\}_i}{h_{pv}} + \{T_a\}_i - T_c \right] \times A_m t_T \quad (40)$$

Exergy analysis

The exergy efficiency of a system is given as

$$\Psi = \frac{E_x}{E_{xsolar}} \quad (41)$$

where E_x is the exergy of the STPV system, which is mainly the electrical power output of the system and is given as²⁹

$$E_x = V_m I_m - \left[1 - \left(\frac{T_a}{T_{pv}} \right) \right] Q \quad (42)$$

where Q is the convective and radiative heat transfer coefficient from PV cell to ambient

$$Q = U_{lc,a}(T_{pv} - T_a) A_m \quad (43)$$

E_{xsolar} is the exergy rate from the solar irradiance in W/m^2 and is given as²⁹

$$E_{xsolar} = \left[1 - \frac{T_a}{T_{pv}} \right] I \Delta t A_m \quad (44)$$

Thermal comfort

Fanger and Toftum³⁰ proposed the numerical model to predict the thermal comfort of people in the 1970s and it is termed as the predicted mean vote index. There are also the ASHRAE thermal scale and Bedford's comfort scale, which use the same number of points but with different semantics. The PMV index is derived for steady-state conditions but can be applied with good approximation during minor fluctuations of one or more of the variables

$$PMV = (0.303e^{-0.036M} + 0.028) \times [(M - W) - (H + E_c + C_{res} + E_{res})] \quad (45)$$

$$PMV = (0.303e^{-0.036M} + 0.028) \times \left\{ \begin{array}{l} (M - W) - 3.05 \times 10^{-3} X \\ \{ 5733 - 6.99(M - W) - p_a \} \\ -0.42X \{ (M - W) - 5815 \} - 1.7 \times 10^{-5} \\ M(5867 - p_a) - 0.0014XM(34 - t_a) \\ -3.96 \times 10^{-8} X f_{cl} X h_c X (t_{cl} - t_a) \end{array} \right\} \quad (46)$$

The thermal comfort of living room considered in this study is calculated using below expression and the values range from 0 to 2 during the sunshine hour and -1 to 1 in non-sunshine hour.

Environmental cost analysis

This analysis is used to evaluate the CO₂ mitigated by the BIPV module on the environment during the operational period and energy pay-back time (EPBT) of the BIPV module. The mitigation of CO₂ emission from the energy-saving potential and corresponding amount of carbon credit potential of the BIPV module is estimated. The CO₂ emission intensity of coal thermal power plant in India is estimated as 2.08 kg/kWh of electricity generation as reported by Agrawal and Tiwari.²⁸ The expression to calculate the mitigation of CO₂ emission is

$$CO_2 \text{ emissions} = \text{Overall electrical energy/Annum} \times 2.04 \left(\frac{kg}{kWh} \right) \quad (47)$$

$$EPBT(\text{Years}) = \frac{E_{in} \text{ kWh}}{E_{out.th} \left(\frac{kWh}{year} \right)} \quad (48)$$

The trading of carbon foot credit is created to curb the effect of greenhouse gases by reducing the carbon foot print. The breakup of embodied energy of each component of fabrication of the BIPV module has been tabulated in Table 2. Total embodied energy for the BIPV module is

Table 2. Embodied energy of different component in BIPV module.

S. no.	Component	Quantity	Energy density	Total embodied energy	
				BIPV (kWh)	BIPV-PCM (kWh)
1	Aluminum frame	1 kg	55.28 kWh/kg	55.28	55.28
2	Copper wire	1 kg	19.61 kWh/kg	19.61	19.61
3	PCM packing layer	1 kg	4.1675 kWh/kg	–	4.165
4	BIPV module (glass-glass)	0.659 m ²	980 kWh/m ²	646	646
Total				720.9	725

Table 3. Initial investment cost of BIPV modules.

S. no.	Material	Cost \$	
		BIPV	BIPV-PCM
1	Window glass	23	23
2	Polycrystalline solar cell	46	46
3	Aluminium frame	23	23
4	Silica gel	3	3
5	Tedlar sheet	–	11
6	PCM	–	30.
7	Labor charges	7.5	7.5
Total investment cost (\$)		102.5	143.5
Annualised unit cost/kWh (\$) (various orientations)			
		South	0.17
		East	0.18
		West	0.2

721 kWh and for BIPV-PCM is 726 kWh. The EPBT is the ratio of the total energy consumed in the production and installation of the system E_{in} to the overall annual thermal energy ($E_{out,th}$) and is calculated using equation (47). The economic analysis of the BIPV and BIPV-PCM systems is calculated and listed in Table 3.

Results and discussion

Solar radiation

The solar radiations falling on vertical surfaces are dependent on the angle incidence and orientation. The solar insolation over horizontal surface and vertical surfaces with respect to azimuth angles are plotted and shown in Figure 5. The solar insolation on horizontal surface and vertical surface kept towards east is denoted as RHS (radiation on horizontal surface) and as RVSE (radiation on vertical surface east). Similarly, for west, north and south are termed as RVSW, RVSN and RVSS, respectively. The ambient temperature and the wind speed measured for various months are plotted in Figure 6. The incident solar radiation on the north orientation building is found to be minimum during winter and maximum during

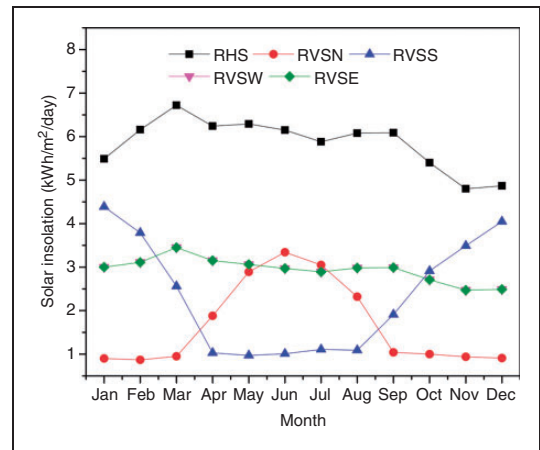


Figure 5. Monthly average solar insolation at horizontal surface and vertical surface for various orientations.

summer while for south orientation, the vertical surface is vice versa. From the graph, it is evident that the solar radiation falling on the vertical surface kept towards the east and west orientation module is almost same.

Transmittance variation

Figure 7 shows the hourly variation of the transmittance of the PV cover glass for vertical

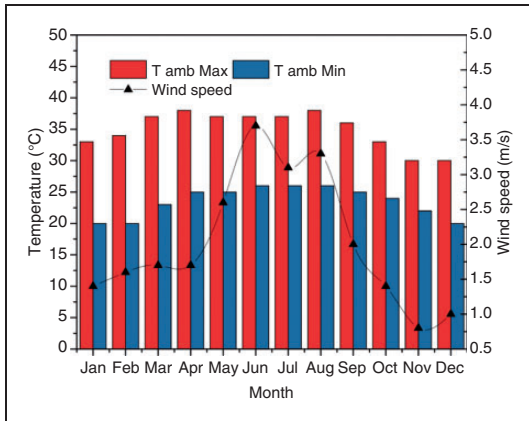


Figure 6. Monthly variation of ambient temperature and wind velocity at Kovilpatti.

surfaces facing north, south, east and west glazing. The transmittance is the function of solar altitude angle and diffused radiation fraction for given thickness. During morning and evening, the transmittance values are maximum for north orientation and minimum for south orientation. During morning hours, when the sun rises, the east orientation receives the maximum, and during evening hours, when the sun sets the west orientation receives the maximum radiation on vertical surface. This is due to the diffused fraction of solar radiation striking on glass surface during morning and evening hours. The diffused radiation fractions are higher due to the air mass.

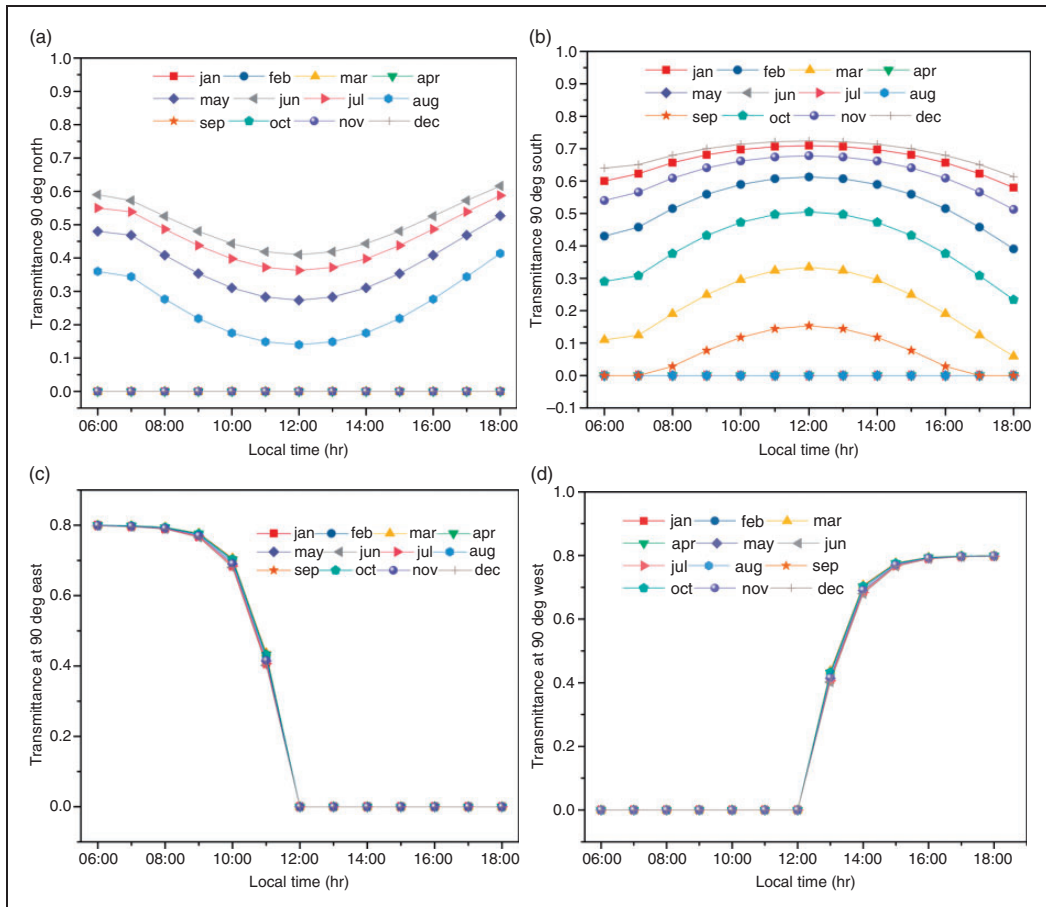


Figure 7. Hourly transmittance variation of 4 mm thickness window glass at vertical surface for various orientations: (a) north, (b) south, (c) east and (d) west.

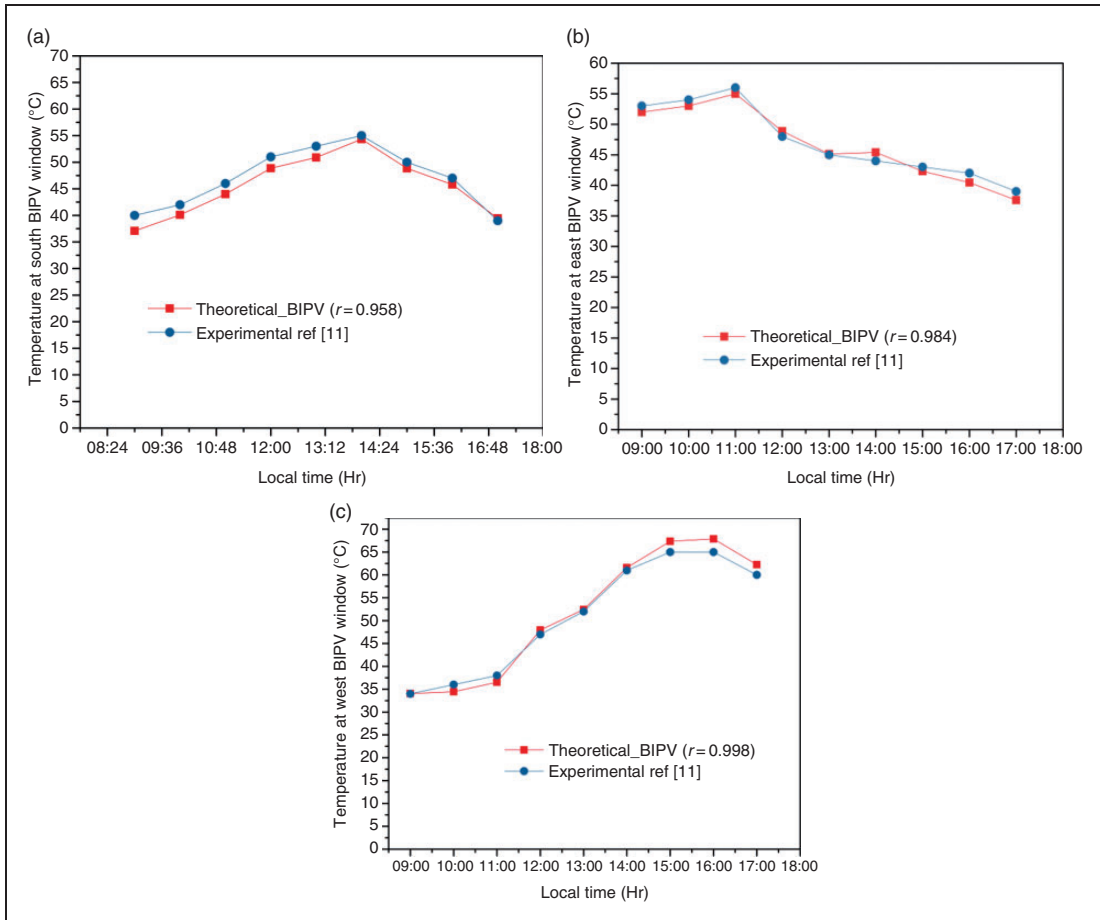


Figure 8. Temperature of BIPV modules at various orientations: (a) south, (b) east and (c) west.

Energy and exergy gain

The surface temperature of BIPV module with and without PCM has been theoretical assessed and validated from the experimental results of Karthick et al.^{11,12} Experimental results of Karthick et al.^{11,12} works are validated with the values of the proposed model and it is shown in Figures 8 to 10. In the current model, the BIPV module predicted surface temperature of the module varies from 2 to 4°C. The predicted surface temperature of the BIPV-PCM maintained the temperature for 4 to 6 h compared to experimental results. It is reported

that the experimental results of BIPV-PCM module surface temperature fluctuated at some points due to the insufficient PCM layers. The predicted result is almost similar to the experimental result and it is evident that the model is suitable to predict the results of BIPV module with and with PCM in hot and humid climatic condition region.

Additionally, deviation in the predicted and experimental results is evaluated using the correlation coefficient (r) and root mean square percent deviation. Generally, these two statistical indicators are used to validate the theoretical and experimental results. The correlation

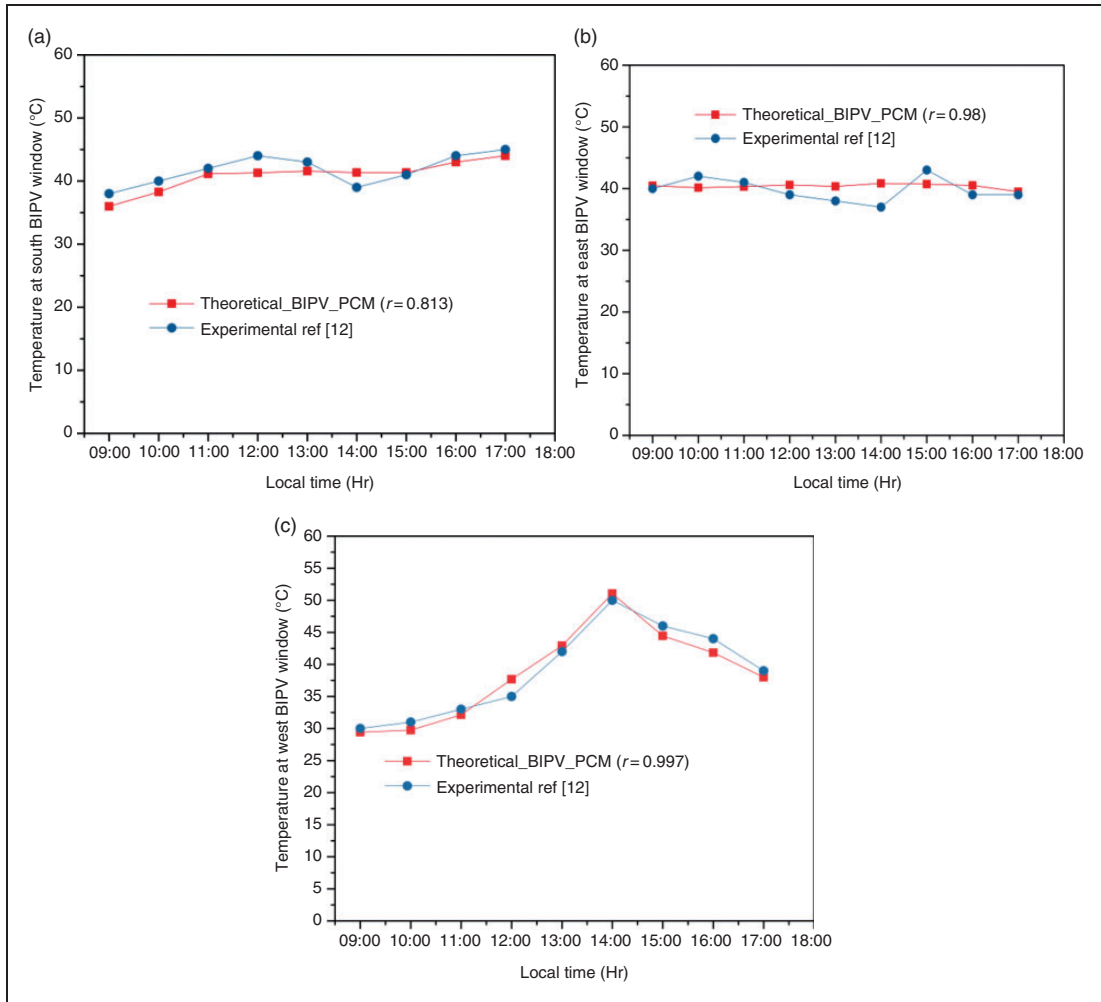


Figure 9. Temperature of BIPV modules with PCM at various orientations: (a) south, (b) east and (c) west.

coefficient of the present model ranges from 0.8 to 0.99; this shows that the proposed model strongly correlates. The thermal imaging camera is used to measure the surface temperature of the module with and without PCM. The net area of the BIPV module is 0.652 m². Figure 11(a) and (b) shows the photograph taken from the thermal imaging camera. It concluded that the predicted surface temperature is almost similar to the measured surface temperature through thermal imaging camera. Figure 12(a) shows the annual thermal and

electrical energy gains of the BIPV and BIPV-PCM. The south orientation BIPV-PCM module obtained the maximum (135 kWh) and the east orientation BIPV-PCM obtained the minimum (110 kWh). Similarly, the annual electrical energy is maximum in BIPV-PCM east orientation and minimum in BIPV west orientation. Figure 13(a) and (b) shows the overall annual thermal energy and exergy for BIPV and BIPV-PCM. The south orientation BIPV-PCM obtained the maximum energy (190 kWh) and exergy (27.3 kWh). Considering the unit cost

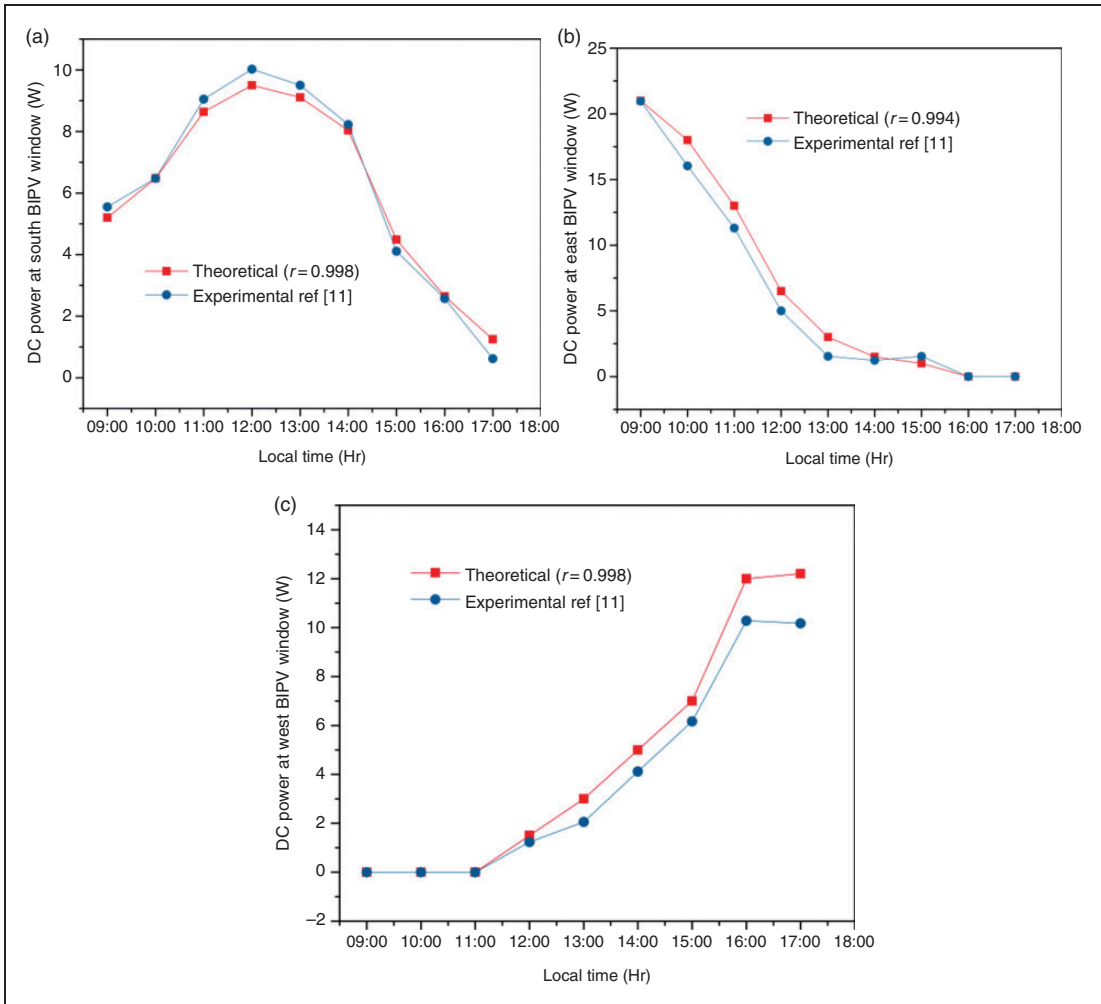


Figure 10. DC power of BIPV modules at various orientations: (a) south, (b) east and (c) west.

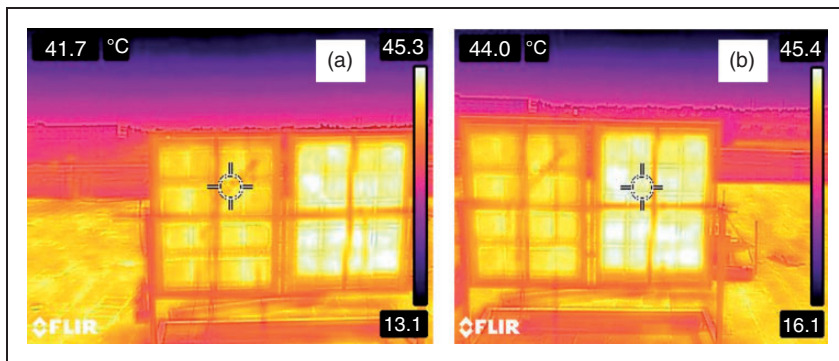


Figure 11. Temperature profiles: (a) BIPV-PCM and (b) BIPV module facing south orientation.

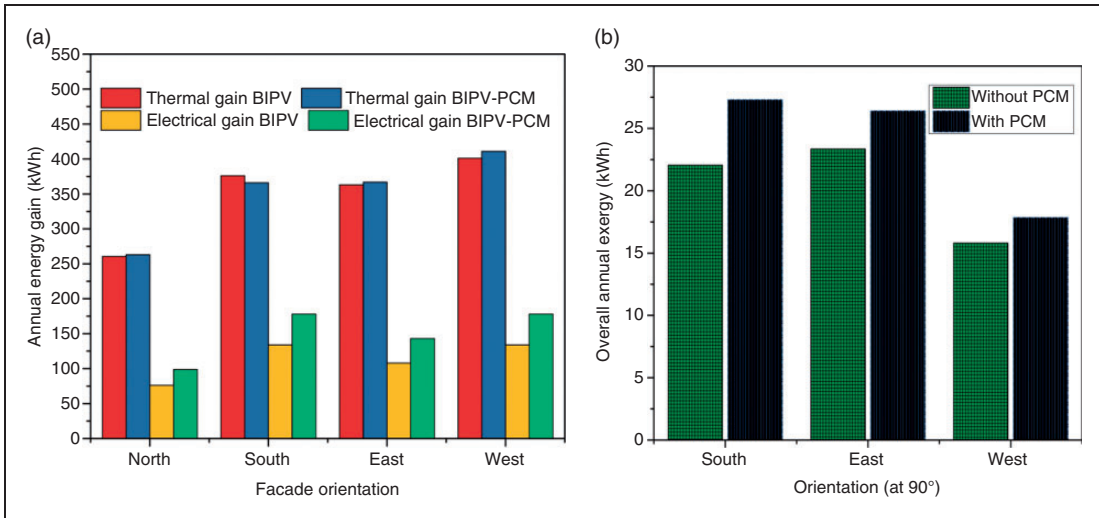


Figure 12. (a) Annual energy gains and (b) overall exergy gains.

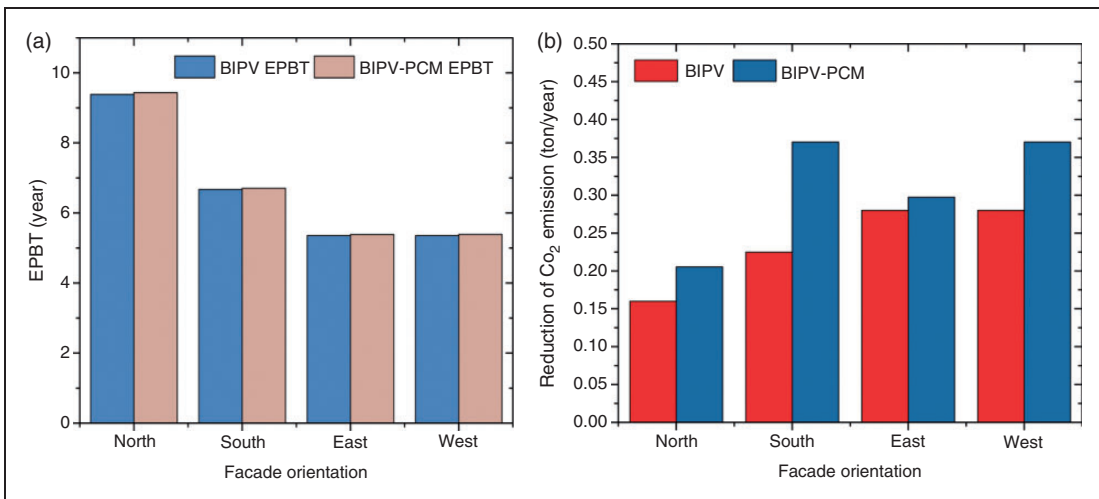


Figure 13. (a) Energy payback time and (b) reduction of CO₂ emission.

of electricity is Rs. 5.5, then the cost of energy produced per annum is $(190 \times 5.5 = \text{Rs. } 1045/-)$ for overall thermal energy. Considering the overall exergy, the cost of energy produced per annum is Rs. 150/-. The carbon dioxide emission reduction due to overall thermal energy produced

in south orientation BIPV is $175 \times 2.04 = 0.357 \text{tCO}_2\text{e}$ (1 ton = 10^3 kg). Considering the CO₂ emission reduction at present being traded at Euro 21/tCO₂e, the CO₂ emission reduction BIPV is $0.387 \times 21 \times 71 = \text{Rs. } 532/\text{annum}$ (where Euro 1 = Rs. 71; October 2016). For the

life time analysis (15 year), the CO₂ reduction by BIPV is $532 \times 15 = \text{Rs. } 7980/-$.

Figure 12(a) and (b) shows the energy payback period of the BIPV modules for various orientations. The energy payback period is lower for BIPV-PCM facing east orientation and higher for BIPV module facing north orientation. The cost of the BIPV and BIPV-PCM system is shown in Table 3. The annualised unit cost of the BIPV system facing south orientation varies from 0.17 to 0.22\$ for south orientation, while for the east and west orientations it varies from 0.17 to 0.25\$ and 0.2 to 0.27\$, respectively.

Conclusion

- In this work, a BIPV module with PCM and without PCM is theoretically modelled and validated with the experimental works of Karthick et al.¹² The transmittance of the solar radiation in the glazing cover has been studied to predict the power generation of the BIPV module.
- In the months of January to March and October to December, the south orientation façade generated more power than north orientation due to the north-facing façade transmittance and solar altitude angles are maximum.
- The annual thermal and electrical energy gains of the BIPV-PCM for the south orientation obtained the maximum (135 kWh) and the east orientation obtained the minimum (110 kWh). Similarly, the annual electrical energy is maximum in BIPV-PCM east orientation and minimum in BIPV west orientation. The south orientation BIPV-PCM obtained the maximum energy (190 kWh) and exergy (27.3 kWh).
- Finally, FLIR thermal imaging camera is used to measure the surface temperature of the BIPV and BIPV-PCM modules. The embodied energy payback period of the BIPV and BIPV-PCM is minimum in the east orientation.


Declaration of conflicting interests

The author(s) declared no potential conflicts of interest with respect to the research, authorship, and/or publication of this article.

Funding

The author(s) received no financial support for the research, authorship, and/or publication of this article.

ORCID iD

A Karthick  <https://orcid.org/0000-0002-0670-5138>

References

1. Ramanan P, Kalidasa Murugavel K and Karthick A. Performance analysis and energy metrics of grid-connected photovoltaic systems. *Energy Sustainable Dev* 2019; 52: 104–115.
2. Karthick A, Kalidasa Murugavel K and Kalaivani L. Performance analysis of semitransparent photovoltaic module for skylights. *Energy* 2018; 162: 798–812.
3. Krishnavel V, Karthick A and Kalidasa Murugavel K. Experimental analysis of concrete absorber solar water heating systems. *Energy Buildings* 2014; 84: 501–505.
4. Hafez AZ, Soliman A, El-Metwally KA, et al. Tilt and azimuth angles in solar energy applications – a review. *Renewable Sustainable Energy Rev* 2017; 77: 147–168.
5. Karthick A, Kalidasa Murugavel K and Suse Raja Prabhakaran D. Energy analysis of building integrated photovoltaic modules. In: *2017 International conference on power and embedded drive control (ICPEDC)*, 2017, Chennai, pp.307–311.
6. Darkwa JDD and Kokogiannakis JG. Thermal management systems for photovoltaics installations. *Solar Energy* 2013; 97: 238–254.
7. Yun GY, Evoy MM and Steemers K. Design and overall energy performance of a ventilated photovoltaic façade. *Sol Energy* 2007; 81: 383–394.
8. Ho CJ, Tanuwijaya AO and Lai CM. Thermal and electrical performance of a BIPV integrated with a micro-encapsulated phase change material layer. *Energy Build* 2012; 50: 331–338.
9. Trinuruk P, Sorapipatana C and Chenvidhya D. Estimating operating cell temperature of BIPV modules in Thailand. *Renew Energy* 2009; 94: 2515–2523.
10. Huang BJ, Lin TH and Hung WC. Sun performance evaluation of solar photovoltaic/thermal systems. *Sol Energy* 2001; 70: 443–448.
11. Karthick A, Kalidasa Murugavel K, Kalaivani L, et al. Performance study of building integrated photovoltaic modules. *Adv Building Energy Res* 2018; 12: 178–194.
12. Karthick A, Kalidasa Murugavel K and Ramanan P. Performance enhancement of a building-integrated

- photovoltaic module using phase change material. *Energy* 2018; 142: 803–812.
13. Royo P, Ferreira VJ, Lopez-Sabiron AM, et al. Hybrid diagnosis to characterise the energy and environmental enhancement of photovoltaic modules using smart materials. *Energy* 2016; 101: 174–189.
 14. Biwole PH, Eclache P and Kuznik F. Phase-change materials to improve solar panel's performance. *Energy Build* 2013; 62: 59–67.
 15. Elarga H, Goia F, Zarrella A, et al. Thermal and electrical performance of an integrated PV-PCM system in double skin facades: a numerical study. *Sol Energy* 2016; 136: 112–124.
 16. Barman S, Chowdhury A, Mathur S, et al. Assessment of the efficiency of window integrated CdTe based semi-transparent photovoltaic module. *Sustainable Cities Soc* 2018; 37: 250–262.
 17. Wang M, Peng J, Li N, et al. Comparison of energy performance between PV double skin facades and PV insulating glass units. *Appl Energy* 2017; 194: 148–160.
 18. Debbarma M, Sudhakar K and Baredar P. Thermal modeling, exergy analysis, performance of BIPV and BIPVT: a review. *Renewable Sustainable Energy Rev* 2017; 73: 1276–1288.
 19. Hasan A, Sarwar J, Alnoman H, et al. Yearly energy performance of a photovoltaic-phase change material (PV-PCM) system in hot climate. *Sol Energy* 2017; 146: 417–429.
 20. Gupta N, Tiwari GN, Tiwari A, et al. New model for building-integrated semitransparent photovoltaic thermal system. *J Renewable Sustainable Energy* 2017; 9: 043504.
 21. Suhatme SP and Nayak JK. *Solar energy principles of thermal collection and storage*, 3rd ed. New Delhi: McGraw Hill Education (India) Private limited, 2013, pp.112–117.
 22. Vats K and Tiwari GN. Performance evaluation of a building integrated semi-transparent photovoltaic thermal system for roof and façade. *Energy Build* 2012; 45: 211–218.
 23. Evans DL. Simplified method for predicting PV array output. *Sol Energy* 1981; 27: 555–560.
 24. Osterwald C. Translation of device performance measurements to reference conditions. *Solar Cells* 1986; 18: 269–279.
 25. Tian Y and Zhao CY. A review of solar collectors and thermal energy storage in solar thermal applications. *Appl Energy* 2013; 104: 538–553.
 26. Hendricks JHC and van Sark HM. Annual performance enhancement of building integrated photovoltaic modules by applying phase change materials. *Prog Photovolt Res Appl* 2013; 21: 620–630.
 27. Gholampour M and Ameri M. Energy and exergy analyses of photovoltaic/thermal flat transpired collectors: experimental and theoretical study. *Appl Energy* 2016; 164: 837–856.
 28. Agrawal B and Tiwari GN. *Building integrated photovoltaic thermal systems for sustainable developments*. Cambridge, UK: The Royal Society of Chemistry, 2011.
 29. Günther E and Hiebler S. Enthalpy of phase change materials as a function of temperature: required accuracy and suitable measurement methods. *Int J Thermophys* 2009; 30: 1257–1269.
 30. Fanger PO and Toftum J. Extension of the PMV model to non-airconditioned buildings in warm climates. *Energy Build* 2002; 34: 533–536.

Appendix

Notation

a	ambient air
f	floor of temperature
g	glass
h_{ceff}	constant
h_i	heat transfer coefficient of room, $W/m^2 K$
h_o	outside heat transfer coefficient, $W/m^2 K$
I_{mp}	maximum current
I_{sc}	short circuit current
$I(t)$	solar intensity W/m^2
K	thermal conductivity, $W/m K$
m	PV module
N	number air changes per hour
P_{max}	maximum power
T	temperature, °C
T_{ref}	reference temperature, °C
T_r	room air temperature
T_{BIPV}	temperature of BIPVW
T_{BIPV_PCM}	temperature of BIPVW_PCM
U_{beff}	constant
V	volume of room, m^3
V_{mp}	maximum voltage
V_{oc}	open circuit voltage

U_{bc}	overall heat transfer coefficient from solar cell to room through glass cover, $W/m^2 K$	α	absorptivity
U_{ra}	overall heat transfer coefficient from room to ambient, $W/m^2 K$	β_c	packing factor or photovoltaic cell coverage ratio
U_{tca}	overall heat transfer coefficient from solar cell to ambient through glass cover, $W/m^2 K$	β_o	temperature coefficient, $^{\circ}C^{-1}$
		λ	reflectivity
		τ	transmissivity
		τ	transmittance of glass